# Sparse antenna array configurations in large aperture synthesis radio telescopes

W.A. van Cappellen, S.J. Wijnholds, J.D. Bregman

ASTRON, P.O. Box 2, 7990 AA, Dwingeloo, The Netherlands

***Abstract* — This paper presents the trade-offs between sparse versus dense and regular versus irregular arrays for the station configuration of the LOFAR Low Band Antenna. The relation between these parameters and the element patterns, station beam patterns, effective area, receiver noise temperature, tapering opportunities and the Field of View (or beam width) are presented. A method is proposed and evaluated to suppress the peak grating lobe level in an aperture synthesis telescope consisting of regular sparse stations.**

***Index Terms* — Antenna arrays, nonuniformly spaced arrays, random arrays.**

## I. Introduction

The international radio astronomy community is currently making detailed plans for the development of a new radio telescope, the Square Kilometer Array (SKA). This instrument will be two orders of magnitude more sensitive than telescopes currently in use and is required to operate from 100 MHz to 25 GHz. A unique SKA antenna concept based on 2-D phased arrays, which comprise the entire physical aperture and which provide multiple, independently steerable, fields-of-view (FoV) is being considered as the European contribution. This "aperture array" concept has hitherto been unavailable for radio astronomy. LOFAR [1] and EMBRACE [2] are the two SKA pathfinder systems for the aperture array technology that are currently being developed for the 10 – 250 MHz and 500 – 1500 MHz bands respectively (see Fig. 1).

In aperture synthesis systems the outputs of widely separated antenna stations are fed into a correlator to synthesize an aperture with a size equal to the largest separation (baseline) between two stations. This is the same principle as applied in today's large radio telescopes like the WSRT and the VLA, but the reflector antennas are replaced by phased array stations. The receptors of such a phased array station can be individual antenna elements but can also consist of arrays itself.

One of the major challenges in the development of aperture array antennas for the SKA is the required ultra-wide frequency bandwidth. An attractive option (from a cost and complexity point of view) is the use of ultra wideband radiating elements, like Vivaldi type elements or active dipole antennas. However, to define the spacing of these elements a fundamental tradeoff between costs and performance has to be made. In the extreme situation, the array is dense at all frequencies, i.e. the inter-element spacing is less than $\lambda/2$ at the highest frequency. Because the frequency bandwidth of such an array is typically two octaves or more, this would lead to a highly over-sampled array at the lower end of the band. Obviously, this is a not a cost effective solution. Therefore, the arrays have to be sparse at the upper part of their band.

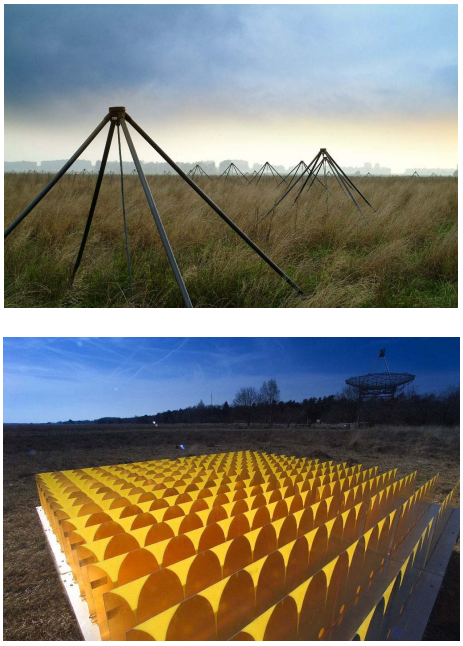

Figure 1. The LOFAR Low Band Antennas (top) and four tiles of an L-band aperture array (bottom).

This paper presents the trade-offs between sparse versus dense and regular versus irregular arrays for the station configuration of the LOFAR Low Band Antenna (LBA). This array consists of 96 dual polarized crossed dipole active antennas in the 10 – 80 MHz band. Using interferometry, all LOFAR station outputs are combined centrally to synthesize the full aperture.

## II. Method

A complete station consisting of 96 dipoles with LNA's and the beam forming network have been simulated with an antenna system simulator developed by ASTRON. It comprises of a MoM based EM simulator and a microwave circuit simulator. Internally, all components are characterized by scattering matrices and noise wave correlation matrices.

With this approach all mutual coupling effects between the antenna elements are taken into account and the elements are properly terminated with the LNA impedance, which is important for the pattern calculations. The S-parameters and the noise parameters (NFmin, Rn, Gamma_opt) of the LNA are simulated and verified with measurements. For the LOFAR LBA a high input impedance (voltage sensing) LNA is used. All results presented below are only for one of the two dipoles. The E-plane of the dipole corresponds to $\varphi = 45°$ in the presented graphs.

## III. Beam Patterns

Since the individual element patterns as well as the complete station beam needs to be accurately calibrated, it is very important that the behavior of the beams is smooth (over scan angle and frequency) such that they can be described by a limited number of parameters.

A clear and well known disadvantage of sparse regular arrays is that grating lobes can enter the visible space. They appear as sidelobes with the same level as the main lobe. They influence the gain of the main lobe significantly and causes strong variations of the main lobe gain as function of frequency and scan angle.

Many methods are being used to reduce the peak level of the grating lobes. Generally, these methods disturb the regularity of the array grid to smear out the grating lobes over all angles. Although the energy is still lost in the grating lobes (reducing the main lobe gain), the smoothness of the main beam over frequency and scan angle is recovered.

A major disadvantage of the irregular grid is that the individual element patterns of the antenna elements can differ significantly. This results in direction dependent complex gains for each antenna making it very hard, especially in practice, to accurately calibrate the system. A less accurate calibration will for example reduce the depth of the nulls that can be realized with the station towards RFI sources. When the antenna pattern variations are known, appropriate corrections can be applied in the beam former to restore the original beam patterns and null depth at the cost of a slightly decreased SNR.

Because a regular grid has much more redundancy, a regular grid is preferred from this point of view. This effect is illustrated in Fig. 2. This figure shows the averaged embedded element pattern and the pattern of a centrally located element of a regular and an irregular array. One can observe that in the regular array, the central element pattern is close to the average element pattern. Although they are not shown, most element patterns resemble this behavior. In the irregular array the situation is different: Only one pattern is shown, but all individual element patterns are different. However, as expected the average pattern is very smooth due to the averaging effect. As such, at the level of the interferometer (i.e. between stations) this smoothness is preferred at the cost of more complicated calibration of the individual stations, leading to less ideal calibration coefficients and thus gain loss.

In a dense regular array side lobes can be reduced by applying a taper. When we make the regular array more sparse grating lobes will appear that have the same intensity as the main lobe. These gratings are unfortunately not affected by the tapering. When the element positions are randomized in the sparse array the grating lobes get randomized as well into many lower ones, roughly in the area where the gratings were. If we now increase the density of the elements in the centre of the array, i.e. apply a space taper, then the sidelobes close to the main lobe are reduced, but the scrambled gratings remain.

Because the beam former is implemented completely digitally, for regular arrays a failure correction technique can be applied to reconstruct the signals of failed elements [3].

Finally, since the number of antenna elements is fixed, an increased spacing between the elements leads to a larger array and consequently a narrower beam. Because the stations are part of an interferometer array, this results in a reduction of the instantaneous field of view. The overall size of the station configuration is therefore limited by the minimum Field of View (the station beam width) requirement and costs of the real-estate and the cables.

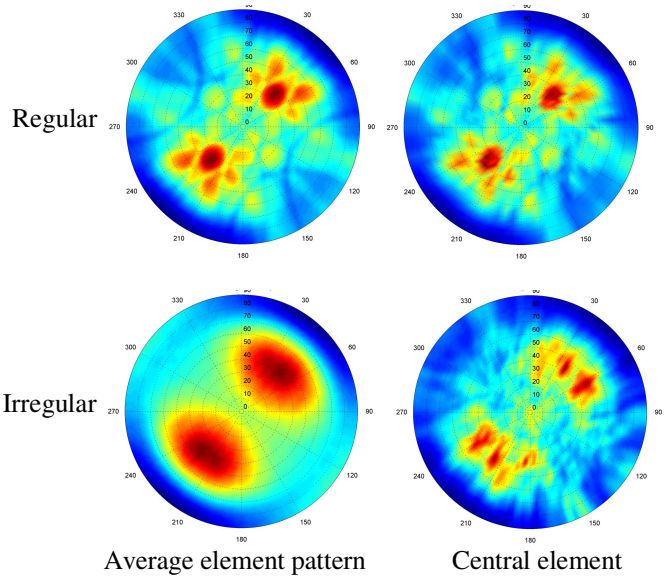


Figure 2. Embedded element patterns of a regular array (top row) and an irregular array (bottom row). The left column shows the average element pattern, the right column shows the embedded element pattern of an element located centrally in the array.

## IV. Receiver Temperature

The radiation efficiency of a single horizontal dipole (or a dipole in a very sparse array) above a conducting ground plane is proportional to its radiation resistance. At the low frequency end, where the dipole is very short with respect to the wavelength, the radiation resistance is in the first order proportional to $\lambda^{-4}$. Therefore, the efficiency drops steeply at

low frequencies while the receiver noise is almost constant, resulting in a reduced sensitivity. However, in more dense arrays the real part of the active element impedance is increased [4] and consequently lowers the receiver contribution to the equivalent system temperature. This is illustrated in Fig. 3: at 25 MHz the dashed line represents an array with a spacing of λ/2. If we compare this with the solid line, which represents an array with a spacing of λ/4 at 25 MHz, the latter has a lower receiver temperature.

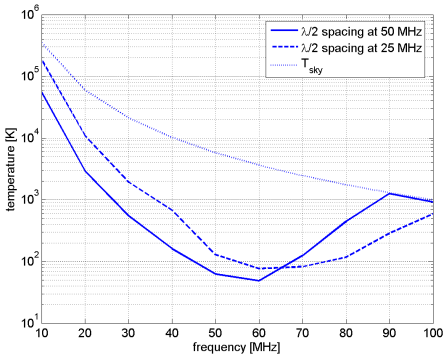


Figure 3. Simulated receiver temperature at broadside of two regular arrays.

## V. Effective Area

For an accurate determination of the effective area full-wave EM simulations are performed. A complete analysis is given in [5]. The effective area of an array (either regular or irregular) with electrically small spacings, i.e. smaller than λ/2, is constant over frequency and smooth over scan angle. If it is assumed that the radiation efficiency is high and the matching is handled correctly then the effective area is roughly equal to the physical area of the array. For electrically larger spacings (for example at higher frequencies), the effective area decreases steeply due to two effects: for very large spacings the dipole array has a constant gain and consequently the gain decreases with the square of the wavelength. On top of this effect comes the appearance of grating lobes which also decrease the effective area in the direction of interest. In Fig. 4 it can be seen that the total decrease of effective area can be more than 10 dB per octave.

Sparse regular arrays are not smooth over scan angle due to the effect of the grating lobes: if the beam is scanned and a grating lobe enters visible space, the main beam effective area can decrease sharply. Irregular arrays have a very smooth effective area over scan angle because the grating lobes are smeared out. This is illustrated in Fig. 5. This figure shows the effective area as function of scan angle. It must be stressed that these are not beam patterns! Every point in this plot represents the effective area of the array when the array is scanned in that particular direction.

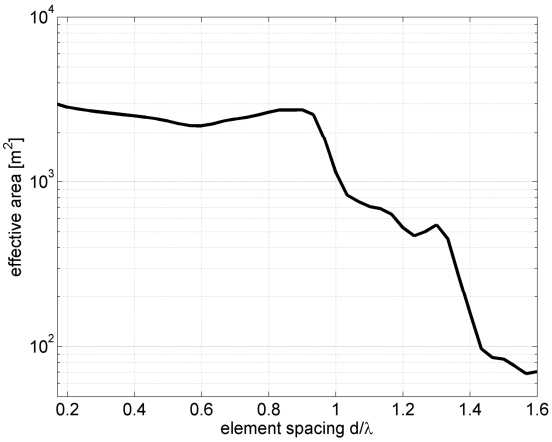


Figure 4. Broadside effective area versus normalised element spacing of a regular array.

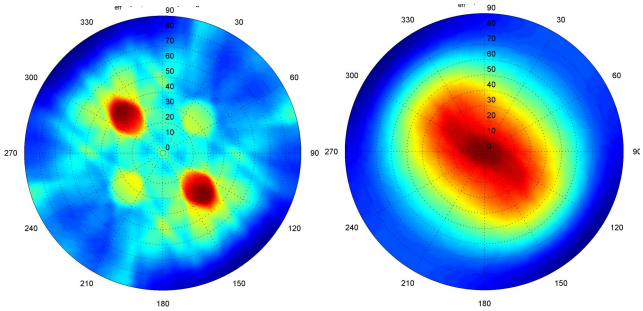

Figure 5. Effective area over all scan angles of a sparse regular array (left) and an sparse irregular array (right).

## VI. Rotated Stations

In an interferometer array, the outputs of every combination of stations are correlated (multiplied). This enables an effective way to reduce the grating lobe peak levels without disturbing the regular grid of the arrays. Consider the two station configurations A and B in Fig. 6. The underlying grid of station B is rotated with respect to the station A. Fig. 6 also shows the beam patterns of these stations with the beam scanned to $\theta = 30°$ $\varphi = 0°$. The main lobe of both stations is unaffected by the rotation, but the grating lobe position of station B is rotated. In the correlation process the patterns of stations A and B are multiplied. Therefore, the grating lobe of station A is suppressed by the sidelobe level of station B and vice versa (Fig. 6 top right).

Fig. 6 (bottom right) finally shows the resulting beam pattern when 8 rotated stations are correlated and summed. The grating lobes now appear as a band of increased sidelobes, 20 dB below the main lobe. It can be concluded that their number has been increased but that their level has been decreased, which is beneficial for our application.

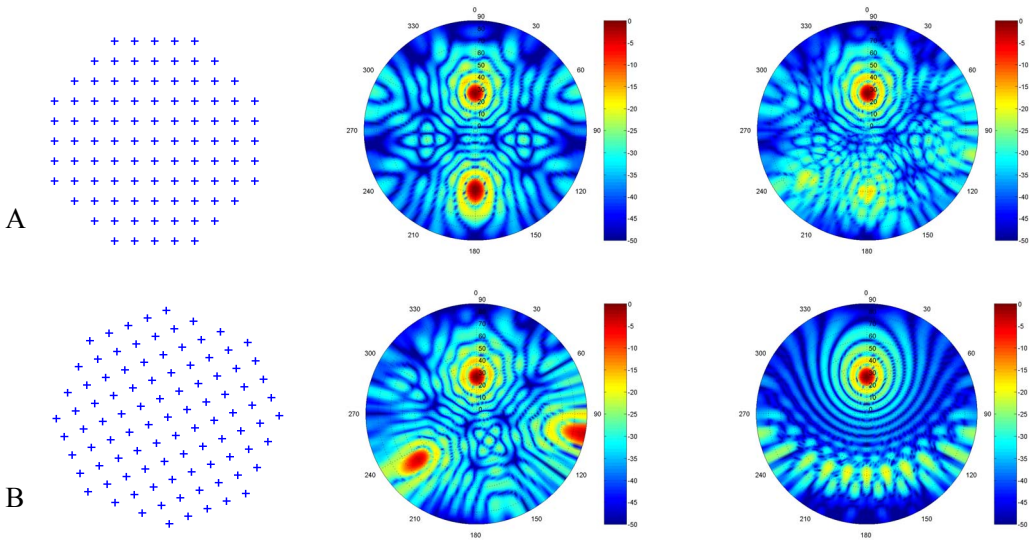


Figure 6. Configurations of two sparse regular array stations (d = 1.2λ) (left), full-wave simulated beam patterns (middle), multiplied patterns of stations A and B (top right) and the summed pattern of 8 cross correlated rotated stations (bottom right).

## VII. Conclusions

Trade-offs between dense versus sparse arrays and regular versus irregular arrays are presented. They are summarized in Table 1.

Given these considerations it has been decided that the first LOFAR station (Core Station 1 or CS1), to be deployed in summer 2006, will use a randomized and exponentially space tapered configuration. The primary motivation of this configuration is the smoothness of both the station beam and the average element beam. The strong variations of the individual element beams challenge the station calibration techniques. CS1 will be used to test these algorithms in practice as a pathfinder for the final LOFAR system.

## References

[1] J.D. Bregman, "LOFAR Approaching the Critical Design Review", *URSI GA 2005*, New Delhi, India, Oct 23 – 25, 2005.

[2] A. van Ardenne , P. N. Wilkinson, P. D. Patel, J. G. Bij de Vaate, "Electronic Multi-beam Radio Astronomy Concept: EMBRACE, The European Demonstrator program for SKA" , in "*The Square Kilometre Array: An Engineering Perspective*", *Springer, 2005.*

[3] R. J. Mailloux, "Array failure correction with a digitally beamformed array," *IEEE Trans. Antennas Propagat.,* vol. 44, pp. 1543 - 1550, December 1996.

[4] B.A. Munk, "*Finite Arrays and FSS*", John Wiley and Sons, 2003.

[5] W.A. van Cappellen, J.D. Bregman and M.J. Arts, "Effective sensitivity of a non uniform spaced phased array of short dipoles", in "*The Square Kilometre Array: An Engineering Perspective*", Springer, 2005.

TABLE I
Summary of Array Characteristics

| | | **Regular** | **Irregular** |
|---|---|---|---|
| | Sidelobes | Lowered by gain taper | Lowered by space taper |
| **Dense** | Grating lobes | No | |
| | Receiver temp | Lower, smooth (angle, freq) | |
| | Effective area | Constant over frequency, smooth over angle | |
| | Element patterns | Depend on position | |
| | Field of View | Large | |
| **Sparse** | Grating lobes | Few high ones | Many low ones |
| | Receiver temp | Higher, not smooth (angle, freq) | Higher, smooth (angle, freq) |
| | Effective area | Steep decrease with wavelength | Steep decrease with wavelength |
| | | Not smooth (angle, freq) | Smooth (angle, freq) |
| | Element patterns | Constant for most elements | Depend on position |
| | Field of View | Smaller | |